2014 IFIP Wireless Days (WD)

Disaster Detection in Magnetic Induction based Wireless Sensor Networks with Limited Feedback

S. Kisseleff *, I. F. Akyildiz **, and W. Gerstacker *
* Institute for Digital Communications, Friedrich-Alexander University (FAU) Erlangen-Nürnberg,
Cauerstr. 7, D-91058 Erlangen, Germany, Email: {kisseleff, gersta}@lnt.de
** Broadband Wireless Networking Lab, Georgia Institute of Technology,
75 5th St. NW, Atlanta, GA-30308, USA, Email: ian.akyildiz@ee.gatech.edu

***Abstract*—The use of magnetic induction (MI) based transmissions in challenging environments has been investigated in various works. Recently, a system model has been proposed, which explains how the MI based transmission channel depends on the chosen system parameters. In order to make the system robust against environmental changes, the system parameters like resonance frequency and modulation scheme need to be properly adapted to the current channel state. It is frequently assumed, that perfect channel state information (CSI) is available at the transmitter and at the receiver. However, in practical systems this knowledge may not always be easily acquired. In addition, a permanent feedback signaling is needed in order to update the CSI at the transmitter, which usually causes interference to the surrounding devices and reduces the energy efficiency. In this paper, we investigate the potential of a recently proposed approach for channel estimation within the MI transmitter circuit without explicit feedback signaling of CSI. This technique seems promising especially for disaster detection in wireless underground sensor networks, which is the main focus of this work.**

Keywords: *Magnetic induction based transmission, wireless underground sensor networks, disaster detection.*

I. Introduction

Magnetic induction (MI) based communication systems are well known in the context of near-field transmissions (cf. [1]), energy harvesting and transfer (cf. [2]), and wireless sensor networks (WSNs) in challenging environments (cf. e.g. [3], [4]). In wireless underground sensor networks (WUSNs), the goal is to establish an efficient wireless communication in the underground medium. Typical applications for such networks include soil condition monitoring, earthquake prediction, border patrol, etc. [5]. Since the propagation medium is soil, rock, and sand, traditional wireless signal propagation techniques using electromagnetic (EM) waves can be only applied for very small transmission ranges due to a high pathloss and vulnerability to changes of soil properties such as moisture [6]. MI-WUSNs make use of magnetic antennas implemented as coils, which are coupled via a quasi-static magnetic field. In previous work (e.g. [7], [8]), some efforts were made to characterize the channel conditions of MI-based transmission, and its potential in different constellations and environments has been thoroughly investigated. In [9] and [10], sets of circuit parameters (resonance frequency and number of coil windings) have been proposed for maximizing the channel capacity of a single point-to-point transmission and the network throughput of a tree-based WUSN, respectively. Modulation approaches for MI-based transmission are discussed in [11], which provides some insight into the MI-specific channel characteristics and corresponding optimized point-to-point transmission schemes.
Disaster detection is one of the target applications of the WSNs. This issue has been addressed in several works on disaster management systems [12]. A proposal for an MI-based rescue network in mines has been given in [13]. The authors investigate several novel techniques (especially the so-called magnetic vector modulation) in order to reduce the latency of the message transport. Furthermore, experimental results are provided based on implemented MI transceivers. However, a fully operational and time-invariant WUSN is assumed, which is not always realistic as we argue in the following. Therefore, the methods proposed in this paper may extend [13], in order to make WUSNs more robust and flexible.
Among different disaster event situations, we distinguish three types of disasters, which are relevant for the operability of the WSNs:

1) All nodes fully functional, signal propagation characteristics unchanged (similar to [13]).
2) All nodes fully functional, environment partly changed (e.g. air $\rightarrow$ soil).
3) Some nodes damaged (possibly destroyed), environment partly unknown.

For many disaster events like fire or toxic pollution, case 1 seems to prevail over the more rare cases 2 and 3. However, in case of explosions, crashes, and cave-ins, the structure of the deployed sensor network may abruptly change. Hence, a reconfiguration procedure needs to be developed for such situations, in order to guarantee the connectivity of the network and the operability of as many functional nodes as possible. As it was shown in [10], for the MI-based WUSNs, which can be employed in such applications, the optimal set of system parameters heavily depends on the distance and environment between any two nodes, on the deployment strategy, and on the traffic load. Hence, if one of the nodes is damaged or if the transmission medium has changed, the currently used set of system parameters (e.g. carrier frequency, packet size, and others) may become suboptimal. Moreover, depending on the topology and on the disaster location, the WUSN may even be disconnected. In such cases, not only the routing of the data flow and the scheduling have to be adjusted (e.g. like it is commonly done using the well-known routing protocols for ad hoc networks [14]), but also a new set of circuit elements

978-1-4799-6606-6/14/$31.00 ©2014 IEEE

has to be employed as part of the reconfiguration procedure. In particular, as proposed in [10], a frequency-switching method may significantly improve the network throughput for case 2.
One of the major problems, which occurs in context with the above discussion, is the necessity of the feedback signaling for alert messaging within the network. Without feedback signaling several sensor nodes may not be notified about the recommended frequency switching or any other adjustments. On the other hand, a permanent signaling of control information occupies additional time slots, thus wasting the resources in terms of bandwidth efficiency. A further drawback of traditional schemes is the waste of energy for transmission of training sequences for channel estimation, such that the lifetime of the small sensor batteries is affected. Taking into account that disaster events related to environmental changes and damage of the nodes are rare, the feedback signaling becomes less and less efficient. Moreover, for a coherent detection of the feedback signal, its slot assignment needs to be available at the node of interest, which is not always possible, especially in case of system reconfiguration. Hence, in this work we investigate the potential of the limited feedback disaster detection and alert messaging for MI-based WUSNs. For this, a novel technique of transmitter-side channel estimation proposed in [15] is utilized. Using this approach, an additional pathloss due to time-varying environmental changes can be predicted based on the phenomenon of the quasi-static magnetic fields, which affect both transmitter and receiver when utilized as parts of an MI channel.
This paper is organized as follows. In Section II, the system model is presented, comprising the basic system components and the network structure. Based on this, the feasibility of disaster detection at the transmitter is investigated in Section III. Section IV shows some numerical results and Section V concludes the paper.

II. System Model

In this work, we utilize the channel and noise models proposed in [9], [10], and [11]. As discussed in several previous works, see e.g. [9], the pathloss and channel capacity of the MI links heavily depend on the chosen system parameters, especially the resonance frequency f_0 and the number of windings N[1]. We follow the principle of the parameter unification, such that all sensor devices are equipped with the same circuit elements, and only one type of devices needs to be implemented. This has been shown to be a good strategy for minimizing the costs of manufacturing and simplifying the hardware design. Hence, the optimization described in [10] can be applied, where the values of f_0 and N and the orientation of the coils are chosen to maximize the network throughput. In particular, a novel approach of interference cancellation using signal polarization in MI-based transmission was proposed in [10]. We note that for the reconfigurability of the network, this interference polarization approach may only be feasible for cases 1 and 2 of the disaster types discussed in Section I, since the data routing does not need to be changed. For the case 3, the polarization of the signal may dramatically reduce the performance, if it is optimized for the outdated scenario. Therefore, we assume that all coil axes of the sensor nodes are parallel and show to the ground surface (vertical axes deployment), such that no polarization algorithm is needed.

[1] N is usually set to its maximum value $N_{\max}$, which complies with the arguments provided in [10].

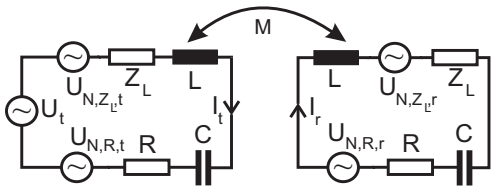

Fig. 1. Information exchange between any two resonant circuits using magnetic induction. Subscripts 't' and 'r' denote transmitter and receiver circuits, respectively. Noise processes are modeled as voltage sources.

Each circuit includes a magnetic antenna (which is assumed to be a multilayer air core coil) with inductivity L, a capacitor with capacitance C, a resistor R (which models the copper resistance of the coil), and a load resistor Z_L, see Fig. 1. The capacitor is designed to make the circuits resonant at the carrier frequency $f_0 = \frac{1}{2\pi\sqrt{LC}}$. The load resistor Z_L is chosen to minimize the power reflection at the receiver. These passive elements are selected according to [10]. The input signal at the transmitting node is modeled as a voltage source U_t. The induced voltage is related to the coupling between the coils, which is determined by the mutual inductance M_i for link i given by [9]

$$M_i = \mu\pi N^2 \frac{a^4}{4r_i^3} \cdot J \cdot G_i, \tag{1}$$

where r_i denotes the distance between the two coils of link i, a stands for the coil radius, N is the number of windings, and μ denotes the permeability of the medium. The polarization factor $J = 1$ is chosen due to vertical axes deployment [9], as discussed above. Obviously, the mutual inductance depends on the system parameters as well as on the environmental parameters, which can vary over space and time. Specifically, the frequency selective attenuation G_i of the field strength in the medium (caused by the so-called eddy currents effect) implies a variation of the transmission channel [9],[16].
The channel transfer function for transmission over link i can be given according to [11]:

$$H_{TxRx,i}(f) = \frac{x_{L,i}}{(x_i + x_{L,i})^2 - 1}, \tag{2}$$

where $x_i = \frac{R + j2\pi fL + \frac{1}{j2\pi fC}}{j2\pi fM_i}$ and $x_{L,i} = \frac{Z_L}{j2\pi fM_i}$.
We focus on the thermal noises caused by the resistors R and Z_L in the transceivers and modeled as voltage sources. The receive noise power density spectrum is given by [10]

$$P_N(f) \approx \frac{1}{2} \frac{4K_B T_K Z_L (R + Z_L)}{\left| R + j2\pi fL + \frac{1}{j2\pi fC} + Z_L \right|^2}, \tag{3}$$

where $K_B \approx 1.38 \cdot 10^{-23}$ J/K is the Boltzmann constant, and T_K is the temperature in Kelvin ($T_K = 290$ K $\approx 17°$ C for our applications). Due to the symmetry and equal system parameters, this noise can be measured at the load impedances in all sensor nodes.
Further parameters related to the signal transmission policies,

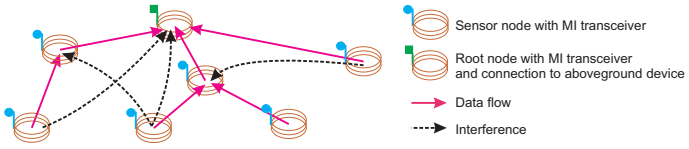

Fig. 2. Example of a simple tree-based MI-WUSN.

like symbol duration T and a smooth band-limited waveform with Fourier transform $H_t(T, f)$ for pulse shaping, are assumed to be constant for all transmission links as well. Adopting the recently proposed three-band transmission scheme for MI channels without relays according to [11], the choice of the optimal symbol duration for the inner sub-band is straightforward, because this parameter is related to the length of the channel impulse response, which should not be longer than 100 taps, cf. [11]. In opposite to previous work on this modulation and transmission scheme, we optimize the widths of the remaining two side-bands, in order to obtain a higher network throughput. Furthermore, a power allocation among the sub-bands needs to be considered. We define the amplification coefficients $A_{i,1}$, $A_{i,2}$, and $A_{i,3}$ for sub-bands 1 to 3, respectively. These coefficients are related to the transmit powers $P_{i,1}$, $P_{i,2}$, and $P_{i,3}$, respectively, given by [9]

$$P_{i,1} = \frac{1}{2}\int_{B_1} \frac{|A_{i,1}\cdot H_t(T_1,f)|^2}{|j2\pi f M_i|}\frac{|x_i + x_{L,i}|}{|(x_i+x_{L,i})^2-1|}\mathrm{d}f \quad (4)$$

for the inner sub-band and similarly for the other sub-bands. Here, B_1 denotes the bandwidth of sub-band 1 and T_1 represents the symbol duration for transmission in this sub-band. Of course, the transmit powers should satisfy the transmit power constraint $P_{i,1} + P_{i,2} + P_{i,3} = P_{\mathrm{tot}}$, where P_{tot} denotes the total available transmit power, which is equal for all nodes.

In this paper, we focus on tree-based networks of N_{nodes} sensor nodes with one sink, which collects the data from all nodes, see Fig. 2. The sink can be implemented as a node, which is connected wirelessly or via wireline with a mobile or removable aboveground device. This network structure is appropriate for most of the target applications with the primary goal of data collection and disaster detection. Each node transmits not only its own information, but also relays all received data from other nodes. We utilize the decode-and-forward relaying concept in this work. Also, we assume that no bit errors occur at the output of the decoder. In order to reduce the number of interferers and improve the available data rate of the links, we design the network based on the minimum spanning tree, which can be found using the Prim algorithm [17]. In order to avoid a performance degradation due to high interference powers from simultaneously transmitting sensor nodes, a multinode scheduling needs to be established, which separates the signals by means of time-division multiple access (TDMA). However, the scheduling issues are beyond the scope of this work, such that the scheduling applied in a real system may differ from the one assumed in our simulations.

For an optimal performance of the network, a throughput related metric needs to be maximized. Following the arguments in [10], we choose the throughput of the bottleneck link as a cost function. Hence, the optimization problem can be formulated as follows

$$\underset{T_j, A_{i,j}\ \forall\{i,j\}}{\arg\max}\ \min_i\{R_{\mathrm{thr},i}\}, \quad (5)$$

where $R_{\mathrm{thr},i}$ denotes the throughput metric for link i given in [10], which incorporates the influence of the interference signals, number of supported data streams, scheduling, and the available data rate at node i. The latter is calculated for a finite symbol alphabet of M-QAM according to [18] for each sub-band and a target symbol error rate SER_t. The corresponding modulation order $M_{\mathrm{mod},i,j}$ for sub-band j is related to the coding gain $K_{i,j}$ of the employed channel code and to the signal-to-noise-plus-interference ratio $\mathrm{SINR}_{eq,i,j}$ at the output of the equalization filter in the receiver node of link i, cf. [11]

$$\mathrm{SER}_t \geq 4\cdot Q\left(\sqrt{\frac{3\cdot \mathrm{SINR}_{eq,i,j}K_{i,j}}{M_{\mathrm{mod},i,j}-1}}\right), \quad (6)$$

where $Q(\cdot)$ is the complementary Gaussian error integral. The available data rate at node i equals

$$R_{d,i} = \sum_{j=1}^{3}\frac{R_{c,i,j}\log_2 M_{\mathrm{mod},i,j}}{T_j}, \quad (7)$$

where $R_{c,i,j}$ is the code rate. In the following, uncoded transmission with $K_{i,j} = 1$ and $R_{c,i,j} = 1\ \forall\ \{i,j\}$ is considered. For receive filtering we employ the whitened matched filter (WMF) [19]. Here, the overall discrete-time channel becomes minimum-phase, and the noise after sampling is white. Since the total transmission channel is frequency-selective, an equalization scheme is needed for the signal detection. In order to avoid further losses in data rate, for our performance investigations we utilize a decision-feedback equalization (DFE) scheme in each sub-band, which minimizes the mean-squared error (MSE) of the output signal.

Since solving the problem (5) in the most computationally efficient way is not the primary goal of this work, we obtain the solution by numerical evaluation of the respective cost function and performing an exhaustive grid search in the feasible parameter set.

III. Disaster Detection in MI Transceivers

A. Channel acquisition at the transmitter

A novel technique of channel acquisition at the transmitter without explicit feedback signaling for magnetic induction based point-to-point signal transmissions has been proposed in [15]. Due to the influence from the receiver coil for link i, the channel transfer function of the distorted signal obtained at the transmitter load impedance can be decomposed into an asymptotical part

$$H_{TxTx,\infty,i}(f) = \frac{x_{L,i}}{x_i + x_{L,i}}, \quad (8)$$

which does not carry any relevant information about the channel due to infinitely long transmission distance assumed for its calculation, and a useful part

$$\Delta H_{TxTx,i}(f) \approx \frac{x_{L,i}}{(x_i + x_{L,i})^3}, \quad (9)$$

which is much more attenuated. Further steps of signal processing, however, are valid only in case of limited interference.

Then, (9) can be equalized and changes in channel attenuation are estimated using one of the two methods proposed in [15]. Basically, the impact of the noise is reduced by averaging within the observation interval. Of course, in case of a high signal attenuation, a very long observation interval is required. Thus, only transmissions in the mid sub-band can be utilized for channel estimation due to its location in the low pathloss region of the spectrum.

In presence of interfering signals with unknown transmitted data, the performance of estimation degrades with the number of interfering nodes, since the corresponding powers are eventually larger than the power of the useful signal at the transmitter node. With increasing number of interferers, the convergence of the averaging becomes slower and slower.

For our further investigations we need to distinguish between three types of network designs:

1) Known scheduling, limited interference: Since in a multihop network the signals can be separated in time domain using a multinode scheduling (as discussed earlier), there may be situations of limited interference for a particular sensor node. Then, the methods proposed in [15] are fully applicable. However, in most of the cases, this can be only achieved, if only one node out of total N_{nodes} sensor nodes transmits at a time. This situation is therefore not desirable due to a very limited network throughput.[2]

2) Known scheduling, multiple interfering nodes: In case of a strong interference from multiple nodes with unknown data symbols it is not possible to properly estimate the channel condition based on the methods proposed in [15] within any reasonable time interval. However, if the slot assignments are perfectly known at the transmitter, the power of the received interference signal can be analyzed and the estimation of the channel attenuation can be successfully carried out using an energy detector, similarly to the concept proposed in [20]. However, during a possible reconfiguration of the network, the scheduling and routing may change, such that the slot assignment may be unknown at the transmitter. Then, even by utilizing an energy detector, no conclusion about the changes in propagation characteristics can be made, since the reference value of the received signal power is unknown. Hence, this scenario is only applicable, if all transmission parameters are adjusted according to the original system design.

3) Unknown scheduling, multiple interfering nodes: The most realistic and general case is the presence of strong interfering signals from multiple nodes with unknown slot assignment. In particular, each node only knows when it has to transmit and to receive data. Other than that, no information about transmission characteristics of the remaining nodes is available. Thus, neither the proposed methods from [15] nor the energy detection can be applied for monitoring the channel conditions in the network. Therefore, in the following we consider this issue and propose a technique, which is based on random access, such that the influence of the interfering signals on channel estimation causes only moderate losses.

[2]If each node transmits its data only in every N_{nodes}th slot, the network throughput decreases by this factor.

B. Proposed method

As discussed earlier, feedback signaling should be avoided in case of unknown multinode scheduling in MI based WUSNs. Therefore, channel estimation can only be done during the own transmission. However, the interference in the same time slot (and same frequency band) prevents from using the whole slot for estimation. In order to avoid a degradation of the network throughput, we propose to split up the time slot in two parts, for pure data transmission (L_{data} symbols) and for data transmission with channel estimation ($L_{\mathrm{ch.est.}}$ symbols), respectively. This ensures, that the throughput decreases at most by factor $\frac{L_{\mathrm{data}}}{L_{\mathrm{data}}+L_{\mathrm{ch.est.}}}$, even if none of the $L_{\mathrm{ch.est.}}$ symbols is used for data transmission. Since the first part is trivially the transmission of the own data, we focus on the more crucial second part, in which a trade-off between data transmission and channel estimation occurs.

In the following, we distinguish between the receiver-side and the transmitter-side packet collisions, where the latter one is only relevant for the channel estimation. In the MI-WUSNs optimized according to Section II, the receiver-side collisions are avoided by the optimal scheduling of interfering signals. On the other hand, this scheduling is sub-optimal for the transmitter-side packet reception, such that packet collisions are inevitable and may disturb the estimation process. Basically, the same packet can be successfully received by the intended receiver node, but may collide with packets from other nodes at the transmitter. In general, we assume that $N_{\mathrm{interferers},i}$ sensor nodes are assigned the same time slot for transmission as node i. We propose to utilize a random medium access strategy with transmitter-side collision detection for the channel estimation related part of the transmitted packets. If no collision is detected, the channel estimation method from [15] is applied to the data packet received at the transmitter in the same way as proposed in Section III-A1. Interestingly, the network throughput benefits from transmitter-side collisions, since more packets are transmitted at the same time. Hence, with an increasing amount of colliding packets at the transmitter the throughput loss due to random access decreases.

For the random access to the channel estimation resources, we select slotted ALOHA as the best suited access scheme, since transmitter-side collisions can only be detected a-posteriori after the full packet transmission. Hence, carrier sensing is not feasible. For slotted ALOHA, the channel utilization, which can be viewed as a fraction of time with successful packet reception on average, is given by e^{-1} [21]. If $(1 + N_{\mathrm{interferers},i})$ nodes including node i try to access the channel during the channel estimation phase, the channel utilization by node i can be given by $(\mathrm{e}\cdot(1 + N_{\mathrm{interferers},i}))^{-1}$. Therefore, the average time for successful channel estimation at the node i increases on average by factor $(\mathrm{e}\cdot(1+N_{\mathrm{interferers},i}))$ compared to channel estimation without random access and without interference.

An example of the random channel estimation access (RCEA) scheme is given in Fig. 3. Here, three users are scheduled by means of TDMA, such that User 1 and 2 transmit in the same time slot and User 3 transmits in disjoint slots. In time slot 1, User 1 and User 2 try to access the channel estimation resource, which leads to a collision. Although no channel estimation is

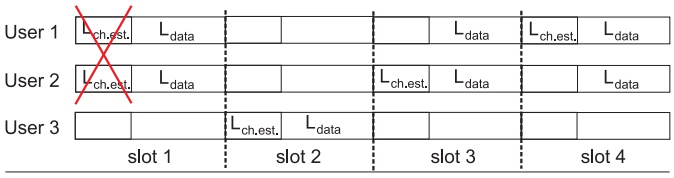

Fig. 3. Example of random access to channel estimation resources.

possible, the throughput in this time slot is maximal, since both parts of the two packets can be received without collision at the respective receivers. In time slot 2, User 3 transmits its data and estimates the channel, since no further interference occurs. In time slot 3, User 1 transmits only in the second part of the slot, such that no collision with User 2 happens. However, the total throughput reduces by $L_{\mathrm{ch.est.}}$ symbols, which are not transmitted by User 1. Similarly, User 1 estimates the channel in slot 4 and User 2 transmits $L_{\mathrm{ch.est.}}$ symbols less.

Depending on the transmission distance and power allocation, the number of symbols needed for a reliable channel estimation may vary from link to link and even exceed $L_{\mathrm{ch.est.}}$. Hence, the estimation process may span several packets, which contribute to the same estimate. Note that only packets without collision can be used. These packets are then processed by means of coherent averaging for estimation of the signal attenuation [15]. The number of symbols needed for channel estimation can be determined by each node independently according to the system requirements, e.g. false alarm probability Pr_{fa}, which represents the probability of an erroneously detected disaster. For the disaster detection, a binary decision using a properly chosen threshold should be made. We choose a threshold, which corresponds to a 6 dB decrease of the received signal power at the respective receiver node. In general, the threshold and the number of symbols for estimation can be jointly optimized, but this issue is beyond the scope of our work.

C. Collision detection

As opposed to the traditional wireless networks with unknown signal propagation characteristics, direct MI transmission based networks (cf. [10]) have a property that different links are characterized by varying attenuation and identical frequency selectivity, as follows from (2). Obviously, the useful part of the received signal at the transmitter utilized for channel estimation shows a different but also constant frequency selectivity, as shown in (9). Therefore, the presence of interference can be easily detected by calculating the cross-correlation between the received signal at the transmitter and a convolution of (9) with the transmitted data known at the transmitter. In addition, the power of interfering signals is usually much higher than that of the useful signal and its presence can be detected even via energy detector. Hence, collisions can be reliably detected.

Furthermore, the "hidden node problem" known in context of the carrier sensing is not an issue for this type of network, since the collision may occur only at the transmitters.

D. Ambiguity of the estimation results

Although it is possible to reliably estimate the channel attenuation by utilizing the proposed methods, a certain ambiguity of the estimation results remains yet unsolved. This ambiguity is caused by the fact, that all nodes can reflect the transmitted signal. Hence, the proposed channel estimation is related not to a single transmission link, but to the whole network. Thus, if the coupling between the transmitter and any distant node is disturbed, this may effect the result of the channel estimation, such that it can not be uniquely interpreted. Since the reflected signal parts depend only on the own transmitted data, we can formulate the total channel transfer function as

$$\Delta H_{TxTx,i,\mathrm{total}}(f) \approx \frac{Z_L \cdot (j2\pi f)^2}{(Z+Z_L)^3} \sum_k M_{i,k}^2, \qquad (10)$$

where $M_{i,k}$ stands for the mutual inductance between node i and node k. Hence, the expectation value of the estimate is related to $\sum_k M_{i,k}^2$ instead of $M_{i,j}^2$ as in point-to-point MI communications [15]. Unfortunately, it is not possible to extract any information about the link of interest from the sum. However, by estimating the changes of the sum, we can estimate the changes of the whole environment around the considered node i. Interestingly, this yields a further benefit of a faster node notification, since the disaster event can be detected even via nodes, which are not linked to the considered node. For the disaster detection, at first, the assumed values of $M_{i,k}$ are determined based on the known positions of the nodes and assumed propagation conditions. Based on this, the assumed value of $Q = \sum_k M_{i,k}^2$ is calculated. Then, Q is estimated based on the received signal at the transmitter. We denote δ the relative deviation of the estimate of Q from the assumed value of Q. In the last step, δ is compared with a properly chosen threshold, as discussed earlier.

E. Disaster detection and network notification

For the alert messaging and network switching, which should be as energy and bandwidth efficient as possible, we propose to not explicitly send the message in the opposite direction of the data flow, because this may either require additional time slots for the feedback signaling or the message might collide with data packets from other transmissions, such that it may not be correctly detected. One of the solutions to this problem is to simply switch to another resonance frequency by connecting the resonance circuit to a different capacitor [10] after disaster detection, which can be easily implemented. Then, no information can be exchanged between transmitter and receiver nodes any more and this can be detected by the surrounding nodes. Of course, the new resonance frequency has to be known at all sensor nodes, in order to ensure the connectivity of the network. For disaster detection and notification in mines, we propose to choose a lower frequency, since the propagation medium may become conductive in case of cave-ins or crashes.

We distinguish between two possible detection scenarios for transmission link i: not functional transmitter or not functional receiver. Not functional means in this context either damaged or switched to another frequency. The first case is trivial, since the receiver knows when to receive the data. Hence, it may wait for a predefined time after the interruption of transmission for a reliable notification. Here, in order to tell the sink node where the disaster happened, the receiver may replace the actual data

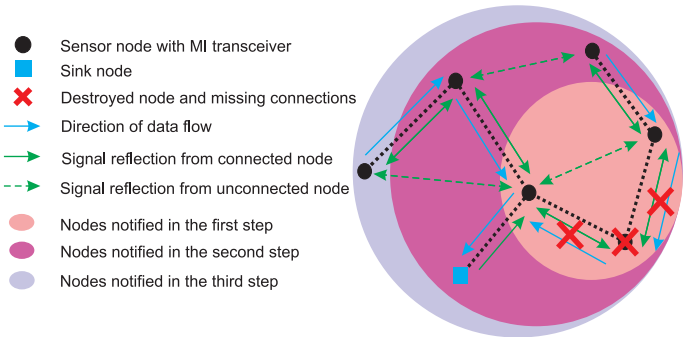

Fig. 4. Example of network notification.

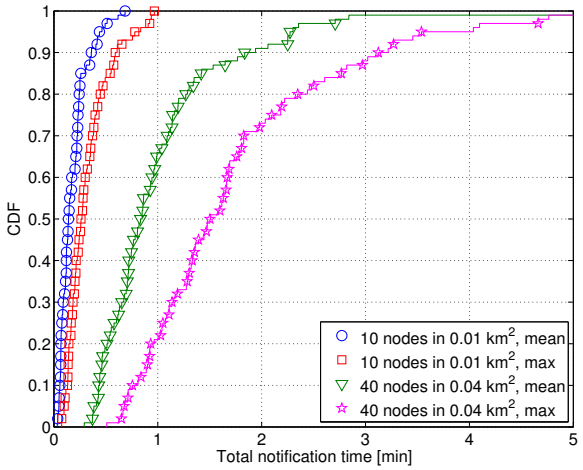

Fig. 5. Cumulative distribution of the network notification time.

to be sent by the event message code, which can be decrypted either by all nodes (as assumed in this work) or by the sink node only. For the second case, shifting the resonance frequency in the receiver prevents the signal reflection at its coil during transmissions at the original resonance frequency, such that $\Delta H_{TxTx,i}(f) \approx 0$. By utilizing the proposed disaster detection approach from Section III-A - Section III-D, this case can be reliably detected by the transmitter node, which then adjusts its own resonant circuit in the same way. Note, that a battery depletion does not trigger the network switching, since the resonance circuit of the corresponding node remains unchanged.
In order to visualize the stepwise network notification, a simple example of a network is shown in Fig. 4. Here, one of the nodes is damaged, such that two transmission links are destroyed. At first, this event is detected by the receiver node of the destroyed link, which is connected to the sink node. This node changes the resonance frequency. The transmitter of the second destroyed link listens to the signal reflections and detects the disaster as well. In the next step, two more nodes and the sink node are notified. In the third step, the remaining node is notified and the network switches completely to the new frequency. We point out, that the decision, to switch or not to switch, is made directly by the particular nodes in a decentralized manner.
After the whole network has been notified, the nodes may start a reconfiguration procedure, which is a well studied issue [14] and therefore not considered here.

IV. Numerical Results

In this section, we discuss numerical results on the performance of the proposed disaster detection and network switching. In our simulations, we assume a total transmit power of $P_t = 10$ mW per sensor node. Within a square field of the size $F_x \times F_x$, a random uniformly distributed set of N_{nodes} sensor nodes is generated for each simulated network. In this set, a root node is selected, which is the closest node to the lower left field corner. We utilize coils with wire radius 0.5 mm, coil radius 0.15 m, and $N_{\max} = 1000$ coil windings. The conductivity and permittivity of dry soil are, respectively, $\sigma_{\text{soil}} = 0.01$ S/m and $\epsilon_{\text{soil}} = 7\epsilon_0$, where $\epsilon_0 \approx 8.854 \cdot 10^{-12}$ F/m [13]. Since the permeability of soil is close to that of air, we use $\mu = \mu_0$ with the magnetic constant $\mu_0 = 4\pi \cdot 10^{-7}$ H/m. For the transmissions through the air (as assumed to be the usual case before the disaster), we use $\sigma_{\text{air}} = 0$ and $\epsilon_{\text{air}} = \epsilon_0$. The target symbol error rate is selected to $\text{SER}_t = 10^{-3}$, and the roll-off factor of the used RRC transmit filter is 0.25.
In order to achieve high data rates even in case of sudden environmental changes, which may trigger the frequency switching [10], we optimize most of the available system parameters for maximizing the network throughput in soil medium in the way discussed in Section II. This includes the analogue filters and frequency bands. However, regarding the pre-disaster channel conditions we assume that through-the-air signal propagation is possible and choose the capacitor, modulation scheme, and signal amplification according to the deployment in non-underground medium. Note that switching between different resonance frequencies does not require additional transceiver devices at the node, since only the capacitor is exchanged.
We utilize a packet length of 500 symbols with $L_{\text{data}} = 450$ symbols and $L_{\text{ch.est.}} = 50$ symbols. Hence, a network throughput loss due to random access of at most 10% can be expected. The number of packets needed for a reliable channel estimation is determined by the respective nodes, such that $\text{Pr}_{fa} = 10^{-4}$ holds for the false alarm probability.
As one of the most important performance measures, we show the total elapsed time, until all nodes are notified about the change in resonance frequency, see Fig. 5. We investigate two scenarios, a small sensor network with $N_{\text{nodes}} = 10$ deployed in 0.01 km^2 ($F_x = 100$ m) and a larger network with $N_{\text{nodes}} = 40$ deployed in 0.04 km^2 ($F_x = 200$ m). For each case, the results are obtained from 100 randomly generated and optimized networks. Then, one of the nodes is set to be malfunctioning and the network switching is simulated under the assumptions provided in the previous sections. Of course, depending on the location of the disaster, the elapsed time varies even for a given network. Therefore, we simulate N_{nodes} scenarios with different malfunctioning nodes for each network and obtain a distribution of the notification time per network. It seems reasonable to consider both the expectation value of the notification time (assuming e.g. equal disaster probability among all nodes) and the maximum notification time, which can be seen as the lower bound for the system performance. Obviously, the small network with 10 nodes is notified very fast due to a small number of hops. Also, the number of interferers

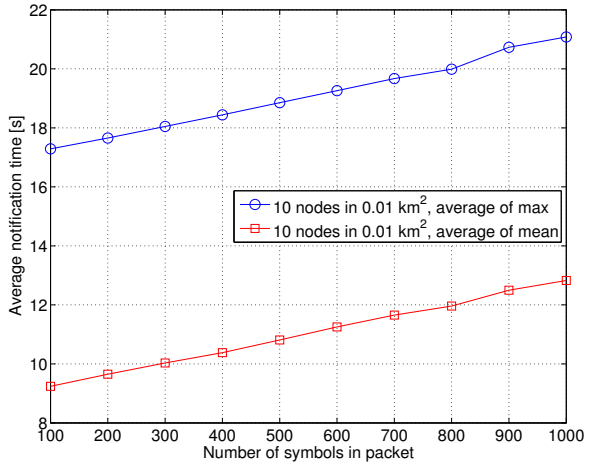

Fig. 6. Average of the mean and maximum notification time.

is lower than with 40 nodes, such that the RCEA is more efficient. With 10 nodes, all networks are notified in less than one minute. With 40 nodes, 99% of networks are notified in less than five minutes. On average over all networks, small networks with 10 nodes need $\approx$ 11 seconds for switching to another frequency. Larger networks with 40 nodes need on average one minute. Of course, there are some extreme cases, where the total notification time exceeds five minutes. Depending on the system requirements, it may be preferable to establish a feedback signaling-aided communication for such cases.

Furthermore, we have observed an average network throughput loss due to the random access of less than 4% for $N_{\text{nodes}} = 10$ and less than 5% for $N_{\text{nodes}} = 40$, which is a negligible penalty for performing a channel estimation and saving energy due to the limited feedback transmissions. This throughput loss is much less than 10% as expected, which is due to the fact, that in several cases the number of interfering data packets is very limited due to the scheduling. Hence, the channel utilization by the node of interest is higher. A distinct reason is that the network throughput benefits from the transmitter-side packet collisions as described before.

In addition, we investigate the influence of the packet length on the notification time for $N_{\text{nodes}} = 10$. For this, we provide the average values of the mean and of the maximum notification time of 100 random networks using different packet lengths, see Fig. 6. Here, the number of symbols for channel estimation $L_{\text{ch.est.}}$ is set to 10% of the packet length. Obviously, with longer data packets the notification time increases, because $L_{\text{ch.est.}}$ is sometimes larger than needed. However, with too short data packets, collision detection may become unreliable.

V. Conclusion

In this paper, a novel approach for disaster detection and node notification in MI based WUSNs with limited feedback signaling has been introduced. The approach is based on the recently proposed transmitter-side channel estimation in MI based communication systems. In order to circumvent the problem of very strong interfering signals during channel estimation, we advocate to employ a part of the transmission slot for a random channel estimation access. Our scheme is especially advantageous for WUSNs, since the network throughput increases with increasing number of packets collided at the transmitter. Hence, the network benefits both from the channel estimation and from the transmitter-side packet collision. Furthermore, we have addressed the problem of ambiguity of the channel estimates using the proposed method and described a possible network notification by simply changing the resonance frequency. Finally, the numerical results show a very good performance in terms of notification time and throughput loss.

References

[1] R. Bansal, "Near-field magnetic communication," in *IEEE Antennas and Propagation Magazine*, April 2004.

[2] A. Karalis, J.D. Joannopoulos, and M. Soljacic, "Efficient wireless non-radiative mid-range energy transfer," *Annals of Physics*, vol. 323, pp. 34–48, January 2008.

[3] Z. Sun and I.F. Akyildiz, "Magnetic induction communications for wireless underground sensor networks," *IEEE Trans. on Antennas and Propag.*, vol. 58, pp. 2426–2435, July 2010.

[4] M.C. Domingo, "Magnetic Indution for Underwater Wireless Communication Networks," *IEEE Trans. on Antennas and Propag.*, pp. 2929–2939, April 2012.

[5] I.F. Akyildiz, W. Su, Y. Sankarasubramaniam, and E. Cayirci, "Wireless sensor networks: A survey," *Comput. Netw. J.*, vol. 38, pp. 393–422, March 2002.

[6] L. Li, M.C. Vuran, and I.F. Akyildiz, "Characteristics of underground channel for wireless underground sensor networks," in *Proc. IFIP Mediterranean Ad Hoc Networking Workshop 2007*, June 2007.

[7] H. Jiang and Y. Wang, "Capacity performance of an inductively coupled near field communication system," in *Proc. of IEEE International Symposium of Antenna and Propagation Society*, July 2008.

[8] J.I. Agbinya and M. Masihpour, "Power equations and capacity performance of magnetic induction communication systems," *Wireless Personal Communications Journal*, vol. 64, no. 4, pp. 831–845, 2012.

[9] S. Kisseleff, W. Gerstacker, R. Schober, Z. Sun, and I.F. Akyildiz, "Channel capacity of magnetic induction based wireless underground sensor networks under practical constraints," in *Proc. of IEEE WCNC 2013*, April 2013.

[10] S. Kisseleff, I.F. Akyildiz, and W. Gerstacker, "Interference Polarization in Magnetic Induction based Wireless Underground Sensor Networks," in *Proc. of IEEE PIMRC 2013 (SENSA Workshop)*, September 2013.

[11] ——, "On Modulation for Magnetic Induction based Transmission in Wireless Underground Sensor Networks," in *Proc. of IEEE ICC 2014*, June 2014.

[12] M. Bahrepour, N. Meratnia, M. Poel, Z. Taghikhaki, and P.J.M. Havinga, "Distributed Event Detection in Wireless Sensor Networks for Disaster Management," in *Proc. of INCOS 2010*, November 2010.

[13] A. Markham and N. Trigoni, "Magneto-inductive networked rescue system (MINERS): taking sensor networks underground," in *Proc. of IEEE IPSN 2012*, 2012, pp. 317–328.

[14] M. Abolhasan, B. Hagelstein, and J.C.-P. Wang, "Real-world performance of current proactive multi-hop mesh protocols," in *Proc. of APCC 2009*, 2009, pp. 44–47.

[15] S. Kisseleff, I.F. Akyildiz, and W. Gerstacker, "Transmitter-Side Channel Estimation in Magnetic Induction based Communication Systems," in *Proc. of IEEE BlackSeaCom 2014*, May 2014.

[16] E.E. Kriezis, T.D. Tsiboukis, S.M. Panas, and J.A. Tegopoulos, "Eddy currents: Theory and applications," in *Proc. of the IEEE*, October 1992, pp. 1559–1589.

[17] R.C. Prim, "Shortest connection networks and some generalizations," *Bell Sys. Tech. J.*, pp. 1389–1401, November 1957.

[18] A. Goldsmith, *Wireless Communications*. Cambridge University Press, 2005.

[19] J.G. Proakis, *Digital Communications*. McGraw-Hill Higher Education, 2001.

[20] L.R. Varshney, P. Grover, and A. Sahai, "Securing inductively-coupled communication," in *Proc. of Information Theory and Applications Workshop (ITA) 2012*, February 2012.

[21] L. Roberts, "ARPANET Satellite System," *Notes 8 (NIC Document 11290) and 9 (NIC Document 11291) available from the ARPA Network Information Center, Stanford Research Institute, Menlo Park, California, USA*.